

Flow dynamics of a tethered elastic capsule

J. D. Berry, J. Carberry, and M. C. Thompson

Department of Mechanical and Aerospace Engineering,

Fluids Laboratory for Aeronautical and Industrial Research (FLAIR),

and Division of Biological Engineering, Monash University, Melbourne, Victoria 3800, Australia

(Received 8 June 2010; accepted 10 January 2011; published online 28 February 2011)

A two-dimensional model of a tethered capsule is used to elucidate the effects of capsule aspect ratio and capsule internal viscosity on capsule dynamics. Over the parameter space examined, the capsule initially elongates out into the flow and then slowly pivots toward the wall as the capsule relaxes to a steady-state shape. The region of the capsule membrane that would come into contact with the wall corresponds with a region of elevated traction-force magnitude. The effect of viscosity is found to be negligible at low shear rates, but at high shear rates, an increase in internal viscosity leads to an increase in the maximum capsule deformation and maximum force on the tether. At low shear rates, capsules with higher aspect ratios experience less force and deformation. Conversely, at high shear rates, capsules with higher aspect ratios experience greater force and deformation. © 2011 American Institute of Physics. [doi:10.1063/1.3553225]

I. BACKGROUND

A critical function of both leukocytes and platelets is their ability to adhere to the vessel wall. A range of specialized adhesive receptors are inherent in platelets and leukocytes, enabling adhesion to ligands present in damaged vessel walls over a wide range of shear rates.^{1,2} The presence of long thin membrane tethers extruded from the surface of leukocytes and platelets undergoing adhesion has been observed in experiments.^{3,4} At a low shear rate of 200 s^{-1} , the leukocyte membrane tether consists of a single bond at the tether tip, and very little overall cell deformation is observed. However, at a higher shear rate of 800 s^{-1} , membrane tethers consisting of multiple bonds at the tether tip have been observed to form with length of $7\text{--}12 \text{ }\mu\text{m}$ ($0.6\text{--}1$ cell diameter) and width of $\sim 2 \text{ }\mu\text{m}$ (0.17 cell diameter).⁵ Schmidtke and Diamond³ observed tethers with mean length of $6 \text{ }\mu\text{m}$ (0.5 cell diameters) over a shear rate range of $100\text{--}250 \text{ s}^{-1}$ with a growth rate of $6\text{--}40 \text{ }\mu\text{m/s}$. Significant overall cell deformation can be observed when the leukocyte tether consists of multiple bonds. Dopheide *et al.*⁴ observed tether formation in platelets and observed that the mean tether length ranged from 3 to $16 \text{ }\mu\text{m}$ ($1\text{--}5$ cell diameters) over a shear rate range of $150\text{--}10\,000 \text{ s}^{-1}$.

Two regimes were noted during tether formation by Evans *et al.* and Heinrich *et al.*, who formed leukocyte tethers using a bio-membrane force probe.^{6,7} At first, the tether was extruded with a linear elastic extension of the cell membrane. After this elastic behavior, a viscous membrane-pulling regime was observed, which is attributed to the dissociation of the bond from the cytoskeleton. The resistive force of the tether was found to depend on the pulling speed in this regime. The authors postulated that the force on the tether exponentially relaxes to a speed-dependent plateau force.

A model of a cell tether was developed by King *et al.*,⁸ who used a boundary-element method to model a rigid spherical body connected to a wall with an elastic tether. The

initial extraction of the tether was modeled using a linearly elastic spring, and the viscoelastic effect of cytoskeletal dissociation was captured using a phenomenological model in which the force on the tether was proportional to the pulling speed. The transition from spring to viscoelastic model was controlled with a stochastic disassociation model. The model was able to capture tether lengths of $\sim 1.5 \text{ }\mu\text{m}$ at a dimensionless shear rate of $\text{Ca} \sim 10^{-3}$, but neglected overall cell deformation and the effect of cytoplasmic viscosity. A similar model was developed by Yu and Shao to examine the effect of simultaneous tether extraction from both the cell surface and the vessel wall, demonstrating that deformation of the vessel wall contributes to the length of the tether.⁹

The only deforming tethered-cell model was developed by Khismatullin and Truskey, who used a volume-of-fluid method to model the leukocyte as a viscoelastic compound drop.¹⁰ The study showed that if the bulk elasticity of the leukocyte is considered negligible, mimicking a weakening of the cytoskeleton, then the cell forms a tether. The main drawback of the method used is that the surface of the cell is not explicitly defined, meaning that forces and stresses on the cell membrane cannot be accurately measured.

Many approaches have been used to define the membrane's response to deformation, including the approach of Khismatullin and Truskey where the cell membrane is assumed to exhibit constant surface tension.¹⁰ Another approach is to consider the cell membrane as area incompressible with finite bending resistance and negligible shear resistance.^{11,12} In other studies, the cell membrane is modeled as an elastic material with negligible bending resistance, finite area dilation, and shear resistance.^{13,14} Other models have considered the effects of both bending and shear resistance.^{15,16}

The tethered-cell models developed have not considered tethering platelets, which are discoidal, and it would be of interest to determine the effect of cell aspect ratio on tethered-cell dynamics. The models either do not consider

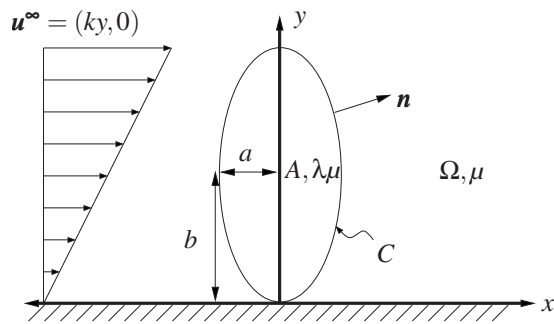


FIG. 1. Schematic diagram of two-dimensional cell model above a plane wall in linear-shear flow. The area A of the cell is kept constant for all cell shapes and the length scale of the problem is $L = \sqrt{ab}$.

overall cell deformability or are not able to measure accurately the forces and stresses acting on the cell. Hence, the present study aims to provide some understanding of the effects of membrane elasticity, internal cell viscosity, and cell aspect ratio on the deformation and forces experienced by a cell tethered to a surface.

In many blood vessels, the inertial forces experienced by cells are very small. In this study, the inertial effects are assumed to be negligible, facilitating the use of the boundary-element method. The boundary-element method provides an explicit definition of the cell interface and has been used to model cell and vesicle deformation, with and without adhesion, in low Reynolds number flows.^{11,12,14} The boundary-element method gives an explicit definition of the cell membrane, allowing an accurate description of forces on the cell surface.

II. PROBLEM STATEMENT

As a first approximation, a blood cell is modeled as a neutrally buoyant, two-dimensional, elastic, elliptical capsule of aspect ratio a/b tethered to a plane wall in linear-shear flow (Fig. 1). The capsule is filled with a Newtonian fluid of viscosity $\lambda\mu$ and is suspended in a fluid of viscosity μ .

By applying a force balance across the elastic interface of the capsule, it can be shown that in the absence of bending moments, the interfacial traction undergoes a discontinuity given by¹⁷

$$\Delta \mathbf{f} \equiv (\boldsymbol{\sigma}^{(1)} - \boldsymbol{\sigma}^{(2)}) \cdot \mathbf{n} \equiv \gamma \kappa \mathbf{n} - \frac{\partial \gamma}{\partial l} \mathbf{t}, \quad (1)$$

where $\boldsymbol{\sigma}$ is the stress tensor, κ is the curvature of the membrane, \mathbf{n} is the normal vector, and l is the arc length along the interface, measured in the direction of the tangent vector \mathbf{t} (Fig. 1). The elastic tension due to membrane deformation, γ , is defined using a constitutive equation relating tension to deformation. For a purely elastic membrane, the relationship between the tension and the deformation can be expressed as¹³

$$\gamma = E \left[\frac{\partial l(t)}{\partial l_0} - 1 \right], \quad (2)$$

where E is the modulus of elasticity of the membrane, $l(t)$ is the arc length along the membrane at time t , and l_0 is the arc

length along the unstressed membrane. Equation (2) ceases to be accurate with finite membrane deformation; however, it is able to capture the capsule's ability to return to its unstressed shape in the absence of flow.¹³ Tests were carried out to ensure that the deformed capsule returned to its unstressed state when the flow was stopped.

For a given position of the interface, the interfacial velocity \mathbf{u} can be found at any point \mathbf{x}_0 on the interface using the nondimensionalized integral equation,¹⁷

$$\begin{aligned} u_j(\mathbf{x}_0) = & \frac{2}{1 + \lambda} u_j^\infty(\mathbf{x}_0) - \frac{1}{2\pi(1 + \lambda)Ca} \\ & \times \int_C \Delta f_i(\mathbf{x}) G_{ij}(\mathbf{x}, \mathbf{x}_0) dl(\mathbf{x}) + \frac{1 - \lambda}{2\pi(1 + \lambda)} \\ & \times \int_C^{PV} u_i(\mathbf{x}) T_{ijk}(\mathbf{x}, \mathbf{x}_0) n_k(\mathbf{x}) dl(\mathbf{x}), \end{aligned} \quad (3)$$

where \mathbf{u}^∞ is the imposed velocity field, \mathbf{n} is the unit normal to the interface pointing into the surrounding fluid, \mathbf{G} is the velocity Green's function of Stokes flow, and \mathbf{T} is the stress Green's function of Stokes flow. The two-dimensional Green's functions for flow bounded by an infinite wall are used in this study, removing the need to mesh the wall surface.¹⁷

The evolution of the capsule interface is governed by the elastic capillary number, Ca , representing the ratio of viscous forces to elastic forces and the viscosity ratio λ . The capillary number, Ca , can be considered as the dimensionless shear rate and is defined as

$$Ca = \frac{\mu k L}{E}, \quad (4)$$

where k is the shear rate and L is the characteristic length, defined here as $L = \sqrt{ab}$.

Equation (3) is solved using the method described by Breyiannis and Pozrikidis,¹³ where the capsule interface is described by a set of marker points, and the shape of the membrane is approximated with natural cubic-spline interpolation. The monotonic parameter s used to parametrize the interpolation is defined as

$$s_k = k, \quad (5)$$

where s_k is the value of s at the k th node. The monotonic parameter s is zero at the tether point, increases in value in the anticlockwise direction around the capsule contour, and reaches a value of s_{\max} back at the tether point. Equation (2) is calculated by fitting a cubic spline to the arc length with respect to the arc length of the unstressed shape. In contrast to Breyiannis and Pozrikidis, who treated the traction as constant over each element, the traction is computed with cubic-spline interpolation across each element. A fourth-order Runge–Kutta–Fehlberg adaptive time-stepping routine is used to determine the new position of the marker points at each time step. For all simulations, the error-control tolerance was fixed at 10^{-6} .

To investigate the effect of capsule shape, the deformation of a capsule is considered for an initial circular capsule,

$a/b=1$, and two initially elliptic capsules, $a/b=0.25$ and $a/b=0.5$. To determine the effect of internal capsule viscosity, a viscosity ratio range of $1 \leq \lambda \leq 10$ has been chosen. Capsules of viscosity ratios higher than 10 were not able to be modeled with sufficient accuracy. The viscosity ratio of a leukocyte is of the order of 10^5 ; however, a trend as the viscosity ratio increases may be able to be discerned, allowing conclusions to be drawn on capsules at higher viscosity ratios. The shear rate range chosen is $0.01 \leq Ca \leq 0.25$. Bending resistance is neglected and the internal area of each capsule is kept constant over the range of aspect ratios. The model presented in this study only captures some of the physics involved with tethered capsules and ignores three-dimensional effects; nevertheless, it represents a first approximation toward a more physiologically consistent model.

To simulate a tether, the node closest to the wall is fixed in position. It was found that imposing shear flow at $t=0$ onto the reference capsule with one node fixed was too unstable to generate equilibrium solutions for some of the parameter space examined. In the initial stages of deformation, a sawtoothlike instability was observed in the velocities of the marker points immediately upstream of the tether point. The size of the instability increased when a finer mesh was used. The constraint of zero velocity applied to the tether point means that marker points immediately upstream move toward the tether, placing this region of the membrane under compression. The presence of the instability may be explained by the tendency of elastic membranes to exhibit buckling under compression, which causes the oscillations of quantities such as curvature and velocity.^{18,19}

To overcome this problem, the capsule was freely suspended at $y/L=0.005$ above the wall and allowed to deform to its maximum extent, without fixing the lowest node of the capsule. The lowest point of the resulting capsule contour was then fixed in position at $(x/L, y/L)=(0, 0.005)$ to represent a tether. For the results presented in this study, all simulations were performed with a mesh size of 256 elements. Accuracy of the method was checked by tracking the area of the capsule over the length of the simulations. Changes of less than 0.5% were evident in most cases. At a viscosity ratio of $\lambda=10$, the change in area was less than 1.5%. For viscosity ratios $\lambda > 10$, the change in area increased significantly, restricting the range of viscosity ratios studied. A series of simulations was carried out to give an estimate of the method's order of accuracy. The order of accuracy of the simulation was found to be approximately $O(N_E^{-2})$, where N_E is the number of elements.

It is reasonable to assume that the relaxation time for an elastic capsule will scale as some function of the viscosity ratio λ . For a liquid drop at a shear rate $Ca \ll 1$, the characteristic time scale for relaxation scales with the viscosity ratio function,²⁰

$$f(\lambda) = \frac{(2\lambda + 3)(19\lambda + 16)}{40(\lambda + 1)}. \quad (6)$$

For viscosity ratios $\lambda \gg 1$, this function reduces to $f(\lambda)=\lambda$. As a consequence, the dimensionless time has been rescaled by λ throughout this study. Because the capsule is anchored

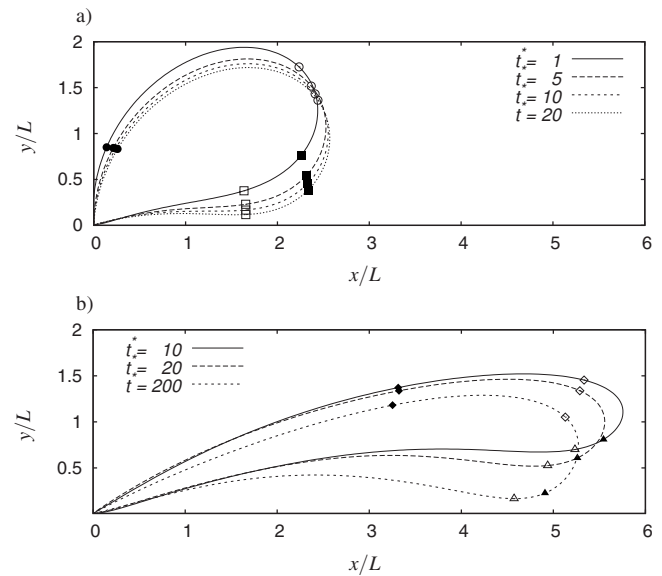


FIG. 2. (a) Capsule contours at different times for a capsule with aspect ratio $a/b=1$ and viscosity ratio $\lambda=1$ at a shear rate of $Ca=0.01$. The symbols present on the capsule contours represent the positions $s/s_{\max}=0.24$ (\square), $s/s_{\max}=0.35$ (\blacksquare), $s/s_{\max}=0.51$ (\circ), and $s/s_{\max}=0.88$ (\bullet). (b) Capsule contours at different times for a capsule with aspect ratio $a/b=1$ and viscosity ratio $\lambda=1$ at a shear rate of $Ca=0.25$. The symbols present on the capsule contours represent the positions $s/s_{\max}=0.51$ (\triangle), $s/s_{\max}=0.55$ (\blacktriangle), $s/s_{\max}=0.66$ (\diamond), and $s/s_{\max}=0.82$ (\blacklozenge). The dimensionless time t^* is defined as $t^*=k(t-t_0)/\lambda$. The flow is from left to right.

to the wall, at equilibrium the membrane velocity will be zero and the internal viscosity will not influence the final shape of the capsule. However, the viscosity ratio may have a significant effect on the maximum deformation and force experienced by the capsule before equilibrium is reached.

III. RESULTS

A. Capsule deformation

The evolution of the capsule contour shown in Fig. 2 is for a capsule of aspect ratio $a/b=1$ and viscosity ratio $\lambda=1$ for shear rates $Ca=0.01$ and 0.25 . It can be seen that the capsule pivots around the tether point and moves closer to the wall as time evolves due to the viscous torque on the capsule generated by the external flow. This suggests that contact with the wall will occur if the tether does not break. It is also apparent that at a high shear rate of $Ca=0.25$, the capsule is initially highly deformed but relaxes as the capsule moves closer to the wall away from the region of higher velocity.

The traction-force magnitude distribution corresponding to the capsule contours of Fig. 2 are shown in Fig. 3. The distribution of the magnitude of the traction force is plotted as a function of the monotonic parameter s used to parametrize the capsule contour. The magnitude of traction on the capsule membrane is highest immediately after tethering, at the point of tethering ($s/s_{\max}=0$). This is in part due to the high hydrodynamic pressure formed in the narrow gap between the anchor point and the wall. As time evolves, the traction-force magnitude immediately downstream of the tether reduces dramatically. The traction-force magnitude in

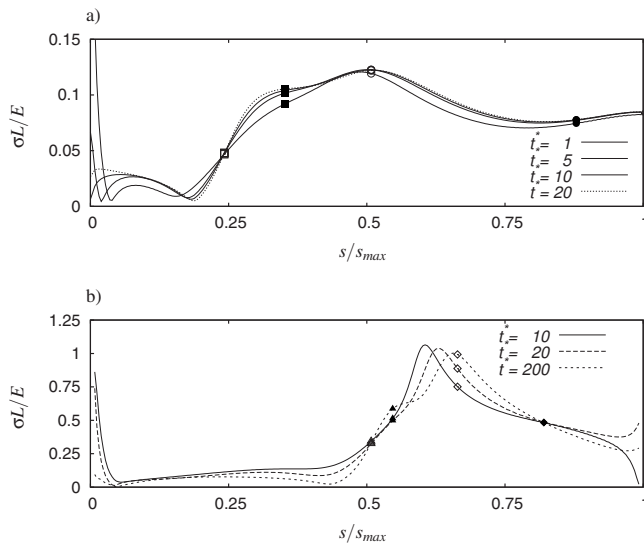


FIG. 3. (a) Distribution of the magnitude of traction force $|\Delta f|L/E$ on the membrane of a capsule with aspect ratio $a/b=1$, viscosity ratio $\lambda=1$ at four different times, at a shear rate of $Ca=0.01$. The symbols present on the distributions represent the positions $s/s_{\max}=0.24$ (\square), $s/s_{\max}=0.35$ (\blacksquare), $s/s_{\max}=0.51$ (\circ), and $s/s_{\max}=0.88$ (\bullet). (b) Distribution of the magnitude of traction force $|\Delta f|L/E$ on the membrane of a capsule with aspect ratio $a/b=1$, viscosity ratio $\lambda=1$ at four different times, at a shear rate of $Ca=0.25$. The symbols present on the capsule contours represent the positions $s/s_{\max}=0.51$ (\triangle), $s/s_{\max}=0.55$ (\blacktriangle), $s/s_{\max}=0.66$ (\diamond), and $s/s_{\max}=0.82$ (\blacklozenge). The dimensionless time t^* is defined as $t^*=k(t-t_0)/\lambda$.

the region of the capsule membrane that would contact the wall if the capsule is tethered for a sufficient period of time is located between the open square and the closed square, in the range of $0.24 \leq s/s_{\max} \leq 0.35$. It is evident that the traction-force magnitude in this part of the membrane increases as the capsule moves closer to the wall. The average traction-force magnitude in this region increases by 20% between $t^*=1$ and $t^*=20$. High regions of traction-force magnitude indicate that the stress on the capsule membrane is high. This observation has ramifications for cell adhesion, where regions of high stress lead to the activation of ligands on the cell surface, increasing the probability of further bonds forming between the cell and the vessel wall. This increase in stress in the region that will contact the wall may provide an explanation of the observation by Ramachandran *et al.* that tether formation in leukocytes correlates with slower, more uniform rolling speeds.⁵ Upon tether breakage, the increase in membrane stress caused by the cell deformation in this region could lead to more ligands becoming activated and thus a greater chance of a new tether forming as this region contacts the wall. It is also clear that the traction-force magnitude on the top of the capsule, located between the open circle and the closed circle in the range of $0.51 \leq s/s_{\max} \leq 0.88$, increases as time evolves, which may increase the probability of other cells adhering to the tethered cell.

The traction-force magnitude on the capsule membrane of the same capsule in a shear flow of $Ca=0.25$ is shown in Fig. 3(b). The capsule experiences much higher traction-force magnitude due to the larger amount of capsule deformation caused by the flow at a high shear rate. It can be seen that the traction-force magnitude immediately downstream

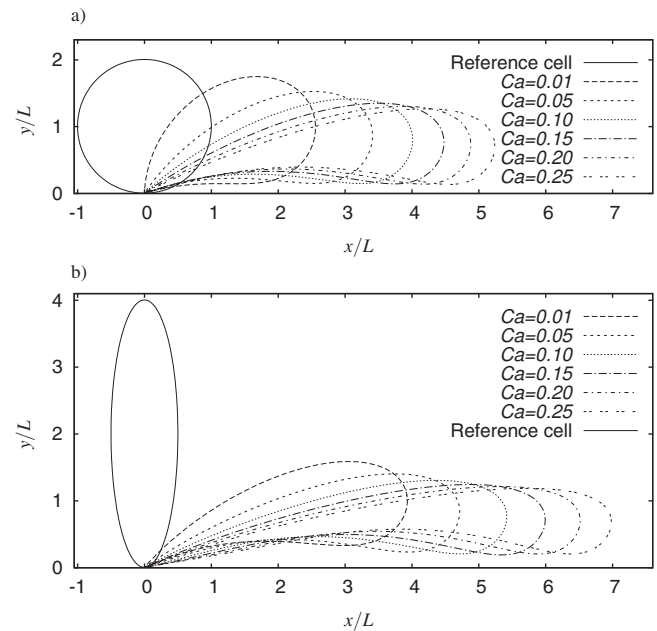


FIG. 4. Equilibrium capsule contours over a range of shear rates for a capsule with aspect ratio (a) $a/b=1$ and (b) $a/b=0.25$. The capsule is determined to be in an equilibrium state when the L_2 -norm of the difference in position between successive time steps falls below 10^{-7} .

of the tether is very high and decreases as time evolves. The region of the capsule membrane, which would come into contact, increases in traction-force magnitude as the capsule moves closer to the wall in the range $0.51 \leq s/s_{\max} \leq 0.55$ (the region between the open triangle and the closed triangle). Again, a portion of the upper part of the capsule contour, located between the open diamond and the closed diamond in the range of $0.66 \leq s/s_{\max} \leq 0.82$, experiences elevated levels of traction-force magnitude as time evolves.

Figure 4 shows a progression of steady-state contours for capsules of aspect ratios $a/b=0.25$ and $a/b=1$ and a viscosity ratio $\lambda=1$ for $0.01 \leq Ca \leq 0.25$. It can be seen that the capsule is drawn out into a flatter, thinner shape along the wall as the shear rate increases. The elliptic capsule is drawn out further along the wall due to its larger initial contour length, forming a longer and thinner tether. Because the internal fluid is at rest when the capsule shape is in equilibrium, the viscosity ratio λ does not affect the shape of the capsule.

B. Tether length

Also of interest is the effect of varying the shear rate, capsule shape, and viscosity ratio on the length of the capsule tether. The length of the capsule in the flow direction has been chosen to represent the tether length, as it can be easily measured as

$$L_{\text{capsule}} = x_{\max} - x_{\min}. \quad (7)$$

The evolution of the length of the capsule in the flow direction shown in Fig. 5 is for a capsule of viscosity ratio $\lambda=1$ and aspect ratios $a/b=1$ and 0.25 . At the lowest shear rate of $Ca=0.01$, the evolution of the tether length reaches a steady-state much quicker than the capsules at the highest shear rate

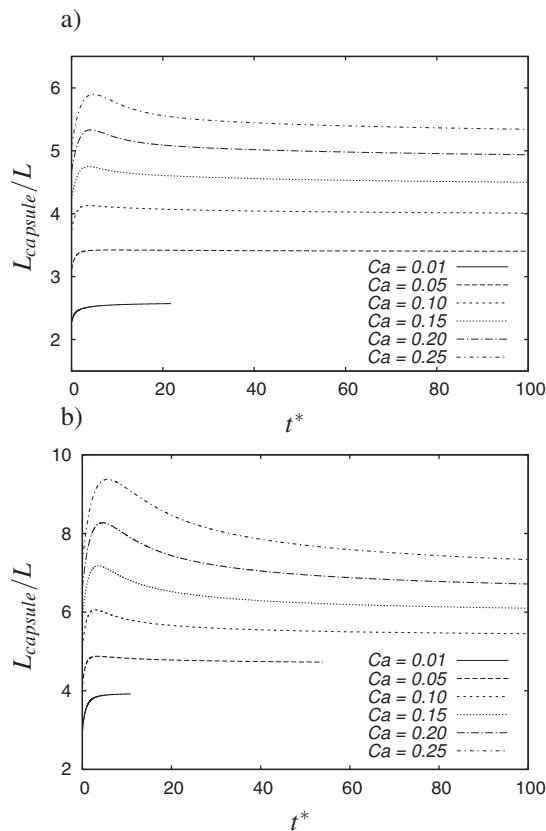


FIG. 5. Evolution of capsule length L_{capsule}/L over a range of shear rates for a capsule of viscosity ratio $\lambda=1$ and aspect ratio (a) $a/b=1$ and (b) $a/b=0.25$. The dimensionless time t^* is defined as $t^*=k(t-t_0)/\lambda$.

of $Ca=0.25$. This is because, at low shear rates Ca , the capsule relaxation time scale is much smaller than the flow time scale and the capsule shape adjusts to the flow very quickly. It is clear that for higher shear rates the elastic response of the capsule is slower to respond to the initial deformation caused by the tethering of the capsule, leading to a rapid increase in a maximum tether length immediately after anchoring the cell. This effect becomes more pronounced as the shear rate increases. Once the maximum value has been reached, the tether length decreases slowly thereafter, as the capsule rotates toward the wall away from the region of higher velocity. The resulting viscous force on the capsule is lower, allowing the capsule to relax to a less-deformed shape. The behavior of the evolution of the tether length is qualitatively similar to that of the model developed by King *et al.*⁸

The effect of viscosity ratio on the capsule length for a capsule of aspect ratio $a/b=1$ at a shear rate of $Ca=0.25$ is shown in Fig. 6(a). The maximum length of the capsule becomes larger as the viscosity ratio increases. To quantify this observation, the maximum capsule length as a function of shear rate for capsules with aspect ratios $a/b=0.25$ and $a/b=1$ is also shown in Fig. 6. The maximum tether length increases with the shear rate, but the rate of increase lessens as the shear rate increases. The rate of increase of the elliptic capsule deformation is greater than that of the circular capsule over all shear rates measured. The maximum tether length is a transient phenomenon, and as such is affected by

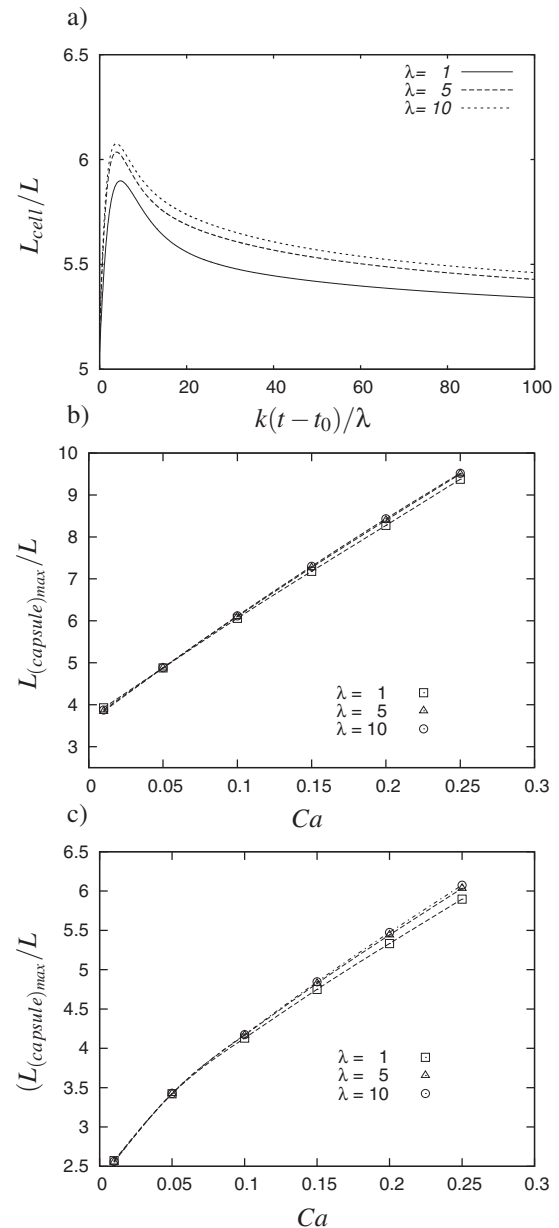


FIG. 6. (a) Evolution of cell length L_{cell}/L over a range of viscosity ratios for a cell of aspect ratio $a/b=1$ at a shear rate of $Ca=0.25$. Maximum capsule length $L_{(\text{capsule})_{\text{max}}}/L$ as a function of shear rate for a capsule with aspect ratio (b) $a/b=0.25$ and (c) $a/b=1$.

the viscosity ratio. It is clear, however, that the effect of varying the viscosity ratio only becomes pronounced at shear rates $Ca \gtrsim 0.1$. Above this shear rate, the maximum tether length increases with viscosity ratio. For large viscosity ratios, the effect of the external flow on the internal fluid initially dominates the elastic response of the capsule, leading to larger maximum tether lengths. It is apparent, however, that the effect of increasing the viscosity ratio diminishes at high viscosity ratios, suggesting that a λ -independent value of maximum tether length exists for viscosity ratios $\lambda > 10$.

C. Force on tethering point

Figure 7 shows the evolution of the total force acting on the capsule tether. This can be calculated using

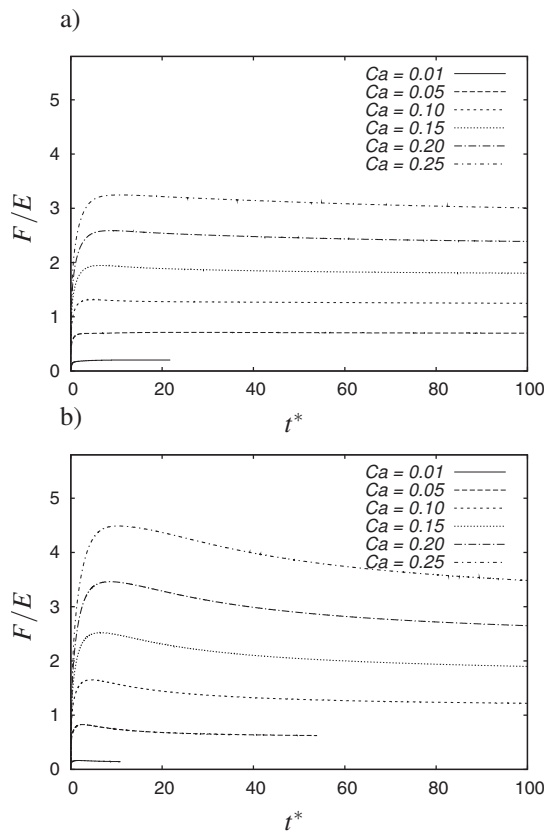


FIG. 7. Evolution of force on the tether F/E over a range of shear rates for a capsule of viscosity ratio $\lambda=1$ and aspect ratio (a) $a/b=1$ and (b) $a/b=0.25$. The dimensionless time t^* is defined as $t^*=k(t-t_0)/\lambda$.

$$|F| = \int_C |\Delta f| dl. \quad (8)$$

The force on the tether increases rapidly to a maximum value for all shear rates and then decreases as time advances. The evolution of the force is qualitatively similar to the results of the model developed by King *et al.*⁸ The maximum peak force observed is $\sim 10\%$ larger than the equilibrium force for the circular cell and $\sim 30\%$ larger than the equilibrium force for the elliptic cell. The presence of a maximum force soon after tether formation suggests that the probability of tether breakage is largest shortly after formation, and the longer a tether is present, the more likely it is that stable adhesion will occur.

The maximum force on the tether becomes more pronounced with increasing viscosity ratio. The initial evolution of the force on the tether at low shear rates agrees qualitatively with the observations of Evans *et al.* and Heinrich *et al.*^{6,7} The authors of the studies postulated that the force response during tether growth exponentially relaxes to a speed-dependent plateau. However, over the range of shear rates examined in this study, it was found that the force initially increases to a maximum value and then decreases thereafter as the capsule pivots about the tether point and moves closer to the wall. The nonmonotonic behavior of the tether force as a function of time can be attributed to the initial dominance of viscous force over the elastic response of the capsule. The capsule initially deforms significantly

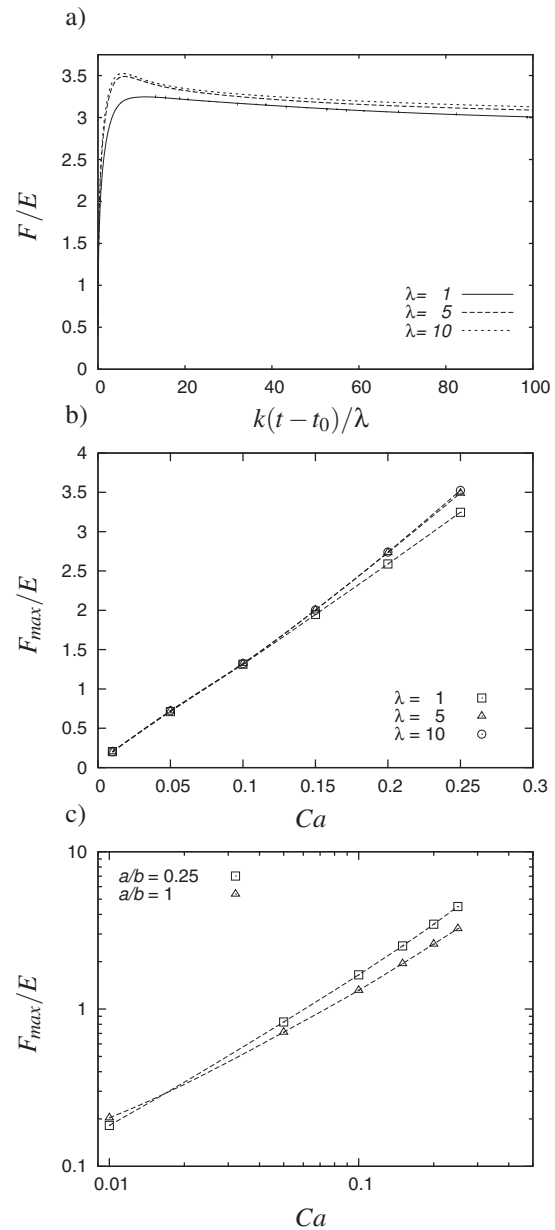


FIG. 8. (a) Evolution of force on tether F/E over a range of viscosity ratios for a cell of aspect ratio $a/b=1$ at a shear rate of $Ca=0.25$. Maximum force on the tether F_{\max}/E as a function of shear rate for a capsule with (b) aspect ratio $a/b=0.25$ and (c) viscosity ratio $\lambda=1$.

because the top surface is moving at a higher velocity than the bottom surface due to its position relative to the wall. The large deformation of the capsule leads to a larger force on the tether point. The elastic response of the capsule then acts to decrease the deformation of the capsule. The torque exerted by the external flow means that the capsule rotates toward the flow, decreasing the viscous force on the capsule and therefore increasing the effect of the elastic response of the capsule. Thus, the overall deformation, and the force on the tether, decreases as the cell pivots toward the wall.

Figure 8(a) depicts the effect of viscosity ratio on the force evolution for a capsule of aspect ratio $a/b=1$ at a shear rate of $Ca=0.25$. Again, it is apparent that an increase in viscosity ratio leads to an increase in the maximum force on the tether. Figure 8 also shows the effect of shear rate on the

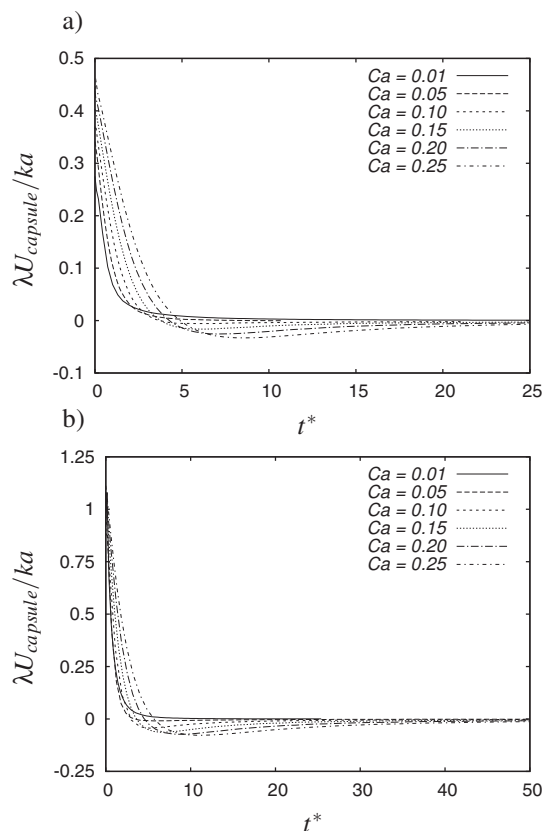


FIG. 9. Evolution of tether growth rate $\lambda U_{\text{capsule}}/ka$ over a range of shear rates for a capsule of viscosity ratio $\lambda=1$ and aspect ratio (a) $a/b=1$ and (b) $a/b=0.25$. The dimensionless time t^* is defined as $t^*=k(t-t_0)/\lambda$.

maximum force acting on the tether on capsules with aspect ratios of $a/b=0.25$ and $a/b=1$. For both aspect ratios, the maximum force on the tether increases with increasing shear rate. It is also clear that the increase in force grows more rapidly as the shear rate increases. Again, the effect of varying the viscosity ratio is only evident at shear rates $Ca \geq 0.1$, where the maximum force increases with increasing viscosity ratio, again attributable to the increased effect of the internal fluid relative to the elastic response of the capsule. However, the effect of increasing λ diminishes with increasing λ . It was also observed that the force on the tether decreases with decreasing aspect ratio for shear rates $Ca \leq 0.15$. At higher shear rates, this effect is reversed and the force increases with decreasing aspect ratio. This effect can be explained by the relative deformations of each capsule. At low shear rates, the elliptic capsule experiences less overall deformation relative to its unstressed shape than the circular capsule and thus experiences less force. At high shear rates, however, the external flow exerts a much greater effect on the elliptic capsule because it initially protrudes further into the flow than the circular capsule. Thus, the transient deformation of the elliptic capsule is more pronounced, leading to a greater force on the tether.

D. Tether growth rate

The growth rate of the tether is shown in Fig. 9. In this study, the growth rate of the capsule tether has been defined

as the magnitude of the velocity of the leading edge of the capsule parallel to the wall. Because the relaxation time scale is inversely proportional to the viscosity ratio λ , it follows that the tether growth rate scales with the viscosity ratio λ . It is clear that the capsule decelerates relatively quickly after tether formation, slowing to zero forward motion in the range of $5 \leq t^* \leq 10$. The time to decelerate to zero velocity increases with decreasing shear rate. At higher shear rates, it is evident that the capsule then moves backward at low velocity for a period before coming to a halt. This period of backward movement corresponds to the capsule rotating toward the wall, minimizing its exposure to the flow and therefore allowing the capsule to relax to a less-deformed shape. It was also observed that the initial tether growth rate increases with the aspect ratio and the capsules with lower aspect ratios take longer to slow to a halt.

IV. CONCLUSIONS

A model of a tethered capsule has been developed to investigate the effects of capsule deformation, internal viscosity, and capsule aspect ratio on the force, length, growth rate, and traction-force magnitude of the capsule. Increasing the shear rate leads to higher overall capsule deformation, longer capsule lengths, larger force on the tether, and higher tether growth rate for all capsules examined in the parameter space.

Immediately after tethering, the capsule experiences a rapid increase in deformation and tether force as the capsule is pulled out into the flow. The deformation caused by the flow is then resisted by the elastic response of the capsule surface and all quantities decrease thereafter as the capsule pivots toward the wall, minimizing its exposure to the external flow. This response is qualitatively similar to the results of the model developed by King *et al.*⁸ The time taken to reach the maximum values of deformation and force scales inversely with the viscosity ratio λ . A region of elevated traction-force magnitude has been found to occur in the part of the capsule membrane that would come into contact with the wall after a sufficient period of time. This finding may in part explain the observation of Ramachandran *et al.* that membrane tether formation corresponds with cell rolling stabilization.⁵ The ligands present on the cell membrane may become activated due to this region of elevated traction-force magnitude, increasing the chances of adhesion with the wall and subsequent tether formation at the leading edge of the cell. A region of elevated traction-force magnitude is also present on the top of the capsule, which provides attractive bonding conditions for other cells to adhere to the tethered cell.

Changing the viscosity ratio of the capsule was found to have negligible effect on all properties measured at low shear rates for capsules with aspect ratio $a/b=1$. Because the relaxation time scale of the capsule is proportional to $1/\lambda$, the tether growth rate should scale linearly with λ . At low shear rates $Ca \leq 0.05$, this was found to hold for all viscosity ratios and aspect ratios considered. At high shear rates, a difference in tether growth rate can be observed at low viscosity ratios, but the difference becomes negligible as the viscosity ratio

increases. At high shear rates, an increase in the maximum capsule deformation, maximum capsule length, and the maximum force on the tether resulted from an increase in viscosity ratio.

It was expected that elliptic capsules would experience higher forces initially as they sit up higher into the flow, but that the force would decrease below that of a circular capsule because it would be able to lie down along the wall. At moderate to high shear rates, $Ca \geq 0.05$, capsules with lower aspect ratios experience greater force and deformation. At lower shear rates, however, elliptic capsules experience less force and deformation than circular capsules, despite sitting up higher above the wall. Elliptic capsules exhibited larger tether growth rates than circular capsules. Capsules with lower aspect ratios were observed to form longer, thinner tethers, but experienced less overall deformation after long tether times. Longer tethers increase the area of the cell exposed to the vessel wall, facilitating the formation of multiple bonds.

The model presented in this study is able to capture larger tether lengths and overall capsule deformation consistent with experimental observations. It is apparent that the aspect ratio of the capsule has a marked effect on the dynamics of the capsule. On the other hand, the effect of viscosity ratio on the transient deformation of the capsule appears to be minimal at viscosity ratios $\lambda > 10$. This result suggests that leukocytes, with an extremely high viscosity ratio of 10^5 , would display qualitatively similar behavior to the idealized model presented in this study. The only major effect of the viscosity ratio is on the time scale of the dynamics, which appears to scale proportional to λ for viscosity ratios $\lambda > 10$.

The above description of a tethered capsule is limited by the choice of Hooke's law to describe the response of the capsule surface to deformation and by the two-dimensional restriction imposed upon the capsule. It is clear that the deformation of a capsule in shear flow is significant, with an increase in the cell contour length of $\sim 100\%$ in the most extreme case considered above. Thus, logical extensions of the present study would be to use a more biologically relevant description of the surface deformation and to implement a three-dimensional deformable model to more accurately capture the physics of cell tethering.

- ¹M. B. Lawrence and T. A. Springer, "Leukocytes roll on a selectin at physiological flow rates: Distinction from and prerequisite for adhesion through integrins," *Cell* **65**, 859 (1991).
- ²B. Savage, E. Saldivar, and Z. M. Ruggeri, "Initiation of platelet adhesion by arrest onto fibrinogen or translocation on von Willebrand factor," *Cell* **84**, 289 (1996).
- ³D. W. Schmidtke and S. L. Diamond, "Direct observation of membrane tethers formed during neutrophil attachment to platelets or P-selectin under physiological flow," *J. Cell Biol.* **149**, 719 (2000).
- ⁴S. M. Dopheide, M. J. Maxwell, and S. P. Jackson, "Shear-dependent tether formation during platelet translocation on von Willebrand factor," *Blood* **99**, 159 (2002).
- ⁵V. Ramachandran, M. Williams, T. Yago, D. W. Schmidtke, and R. P. McEver, "Dynamic alterations of membrane tethers stabilize leukocyte rolling on P-selectin," *Proc. Natl. Acad. Sci. U.S.A.* **101**, 13519 (2004).
- ⁶E. Evans, V. Heinrich, A. Leung, and K. Kinoshita, "Nano- to microscale dynamics of P-selectin detachment from leukocyte interfaces. I. Membrane separation from cytoskeleton," *Biophys. J.* **88**, 2288 (2005).
- ⁷V. Heinrich, A. Leung, and E. Evans, "Nano- to microscale dynamics of P-selectin detachment from leukocyte interfaces. II. Tether flow terminated by P-selectin dissociation from PSGL-1," *Biophys. J.* **88**, 2299 (2005).
- ⁸M. R. King, V. Heinrich, E. Evans, and D. A. Hammer, "Nano-to-micro scale dynamics of P-selectin detachment from leukocyte interfaces. III. Numerical simulation of tethering under flow," *Biophys. J.* **88**, 1676 (2005).
- ⁹Y. Yu and J. Y. Shao, "Simultaneous tether extraction contributes to neutrophil rolling stabilization: A model study," *Biophys. J.* **92**, 418 (2007).
- ¹⁰D. B. Khismatullin and G. E. Truskey, "Three-dimensional numerical simulation of receptor-mediated leukocyte adhesion to surfaces: Effects of cell deformability and viscoelasticity," *Phys. Fluids* **17**, 031505 (2005).
- ¹¹I. Cantat and C. Misbah, "Lift force and dynamical unbinding of adhering vesicles under shear flow," *Phys. Rev. Lett.* **83**, 880 (1999).
- ¹²S. Sukumaran and U. Seifert, "Influence of shear flow on vesicles near a wall: A numerical study," *Phys. Rev. E* **64**, 011916 (2001).
- ¹³G. Breyiannis and C. Pozrikidis, "Simple shear flow of suspensions of elastic capsules," *Theor. Comput. Fluid Dyn.* **13**, 327 (2000).
- ¹⁴S. K. Doddi and P. Bagchi, "Three-dimensional computational modeling of multiple deformable cells flowing in microvessels," *Phys. Rev. E* **79**, 046318 (2009).
- ¹⁵H. Noguchi and G. Gompper, "Shape transitions of fluid vesicles and red blood cells in capillary flows," *Proc. Natl. Acad. Sci. U.S.A.* **102**, 14159 (2005).
- ¹⁶I. V. Pivkin and G. E. Karniadakis, "Accurate coarse-grained modeling of red blood cells," *Phys. Rev. Lett.* **101**, 118105 (2008).
- ¹⁷C. Pozrikidis, *Boundary Integral and Singularity Methods for Linearized Viscous Flow* (Cambridge University Press, Cambridge, UK, 1992).
- ¹⁸E. Lac, D. Barthés-Biesel, N. A. Pelekasis, and J. Tsamopoulos, "Spherical capsules in three-dimensional unbounded Stokes flows: Effect of the membrane constitutive law and onset of buckling," *J. Fluid Mech.* **516**, 303 (2004).
- ¹⁹E. Lac and D. Barthés-Biesel, "Deformation of a capsule in simple shear flow: Effect of membrane prestress," *Phys. Fluids* **17**, 072105 (2005).
- ²⁰L. G. Leal, *Advanced Transport Phenomena* (Cambridge University Press, New York, 2007).